JJMIE

Volume 16, Number 1, January. 2022
ISSN 1995-6665
Pages 1 - 9

Jordan Journal of Mechanical and Industrial Engineering

Modeling and Analysis of Relationship Between Flow Characteristics and Efficiency of Reciprocating Porous Medium Burner

Boxue Zhong[1*], Weihua Li[2]

[1]Department of Safety Supervision, Preparatory Office, Datang Baoding Co-generation Power Plant, Baoding 071051, China
[2]School of Energy Power and Mechanical Engineering, North China Electric Power University, Baoding 071003, China

Received 14 July 2021 Accepted 29 December 2021

Abstract

When the relationship model between flow characteristics and efficiency of reciprocating porous medium burner is built by energy spectrum analysis method, it is disturbed by a large number of factors affecting combustion efficiency, so it is impossible to accurately analyze the relationship between flow characteristics and efficiency of the burner. A new relationship model between flow characteristics and efficiency of reciprocating porous medium burner is constructed. According to the symmetry of reciprocating porous medium burning system structure and the periodic exchange characteristics of internal gas flow, a physical model of reciprocating porous medium burning system is constructed. On this basis, a reciprocating porous medium burner is established. After giving the initial boundary conditions of the model equation, the finite volume method is used to discretize the model equation, boundary conditions and calculation area. The Gauss-Seidel iteration method is used to solve the mathematical model, and the relationship between the flow characteristics and efficiency of the reciprocating porous medium burner is analyzed. The experimental results show that the model can effectively analyze the relationship between flow characteristics, such as reversal half cycle, gas calorific value, secondary air ratio and efficiency in reciprocating porous medium burner, and the stability of the model is strong. The analysis time is less than 0.5 s.

Keywords: Reciprocating; Porous medium; Burner; Flow characteristics; Efficiency; Modeling analysis;

1. Introduction

With the development of society and economy, energy crisis and environmental pollution are becoming more and more serious. People's voice for energy conservation and environmental protection is getting higher and higher [1]. The development of clean energy and the efficient use of energy play an important role in promoting and guaranteeing the sustained, rapid and healthy development of the national economy, improving the environment and the quality of people's lives. Controlling the use of highly polluted energy, developing the utilization of clean energy, and improving the effect of energy conservation are to greatly increase the use of energy, which has become one of the researches focuses of energy researchers since the 1990s [2, 3].

Environment is the source of human life and survival. However, with the development of the world economy, environmental problems are becoming more and more serious, threatening the survival and development of mankind. Nowadays, human beings are faced with three major environmental problems: acid rain, greenhouse effect and ozone layer damage. The harm of acid rain is getting worse and worse, and almost all over the world [4, 5]. According to a survey conducted by the Economic Commission for Europe (UNECE) and the United Nations Environment Programme in 1989, acid rain has been harmful to 28 countries in Europe, and 50 million hectares of 110 million hectares of forests in Europe have become fragile and withered due to acid rain; In the United States, according to Environmental Protection Agency (EPA) estimates, acid rain has corroded up to 5 billion United States (US) dollars in 17 states since 1985. In China, acid rain has been the trend of development, and the acidity of rainfall has been increasing from south to north. The economic losses caused by acid rain are also increasing year by year. Soil in some areas is gradually increasing. Acidification is a serious pollution problem in agriculture. According to rough estimates, the area of farmland polluted by acid rain in the mid-1980s has reached 40 million mu, resulting in economic losses of more than 1.5 billion yuan per year. In addition, some parts of China also suffer from forest and water hazards, which seriously threaten the ecological balance of [6-10].

Reciprocating porous medium combustion has higher advantages than other combustion technologies in improving combustion efficiency, expanding flammability limit, saving fuel, improving environment and disposing of all kinds of garbage and waste [11-14]. It is a combustion technology with high combustion efficiency and low pollution emission. This combustion technology is an effective and practical combustion method in enhancing combustion and emission control. Therefore, the relationship between flow characteristics and efficiency of

* Corresponding author e-mail: boxuezhong@126.com.

reciprocating porous medium burner is analyzed by modeling in order to improve fuel efficiency and reduce environmental pollution.

2. Modeling and Analysis of Relationship Between Flow Characteristics and Efficiency of Reciprocating Porous Medium Burner

2.1. Establishment of physical model

According to the symmetry of the structure of reciprocating porous medium burner and the periodic interchangeability of the gas flow direction in the system, the burner is simplified [15-18]. The physical model shown in Figure 1 is established, which is divided into combustion zone and regeneration zone. The combustion zone and regeneration zone are cylinders, and the burner zone are foam ceramic tile with high porosity, the regenerator area is a regenerative sphere or honeycomb regenerator with low void ratio, and the length of the combustion heat transfer area is x_e; The gas flow area [19] on the outside of the two ends of porous medium is one-twentieth of the length of the porous medium area, and the total length is L. In order to prevent the burner from tempering, a heat dissipation aluminium ring jacket with a length of 40 mm is installed outside the burner at the entrance of some premixed gases [20-22]. The igniter is located at 2/3 of the burner length.

During the first half period t_{hp1}, some premixed gas enters the burner from upstream of the burner at a flow rate of u_1 and initial temperature of T_0. At the same time, the heated secondary air enters the burner at a flow rate of u_2 and a temperature of T_2. It joins the primary air and combusts after ignition by the igniter. The combustion product passes through heat storage. The downstream of the regenerator is excluded [23, 24]. The solid line in the figure shows the direction of gas flow in the first half cycle. In the second half cycle t_{hp2}, the premixed gas stops supplying. The secondary air enters from the downstream of the regenerator at a flow rate of u_2 and an initial temperature of T_0. After heating in the regenerator area and the porous medium combustion area, it flows out of the middle cross-pipe mouth. It can also be seen in the figure that the distance between the premixed gas inlet upstream of the burner and the connecting point of the middle cross-pipe is relatively small compared with the whole burner, and the proportion of the premixed gas inlet in the whole calculation area is relatively small [25]. The influence of the incoming flow of the fresh premixed gas and the heated secondary air in this section can be neglected. Therefore, in the first half of the model processing, it can be considered that the primary and secondary air has been premixed before entering the system from the premixed gas inlet upstream of the burner [26]. Similarly, in the second half of the cycle, the outflow of secondary air can also be considered as outflow from the upstream middle cross-pipe of the burner. In this way, the physical model can be simplified to one-dimensional problem in the first and second half cycle.

2.2. Establishment of mathematical model

2.2.1. Establishment of model equation

According to the results of the physical model built in Section 2.1, an axial coordinate system x is established. As shown in Figure 1, for the combustion reaction process of reciprocating porous burner in the first half cycle, a micro-element is selected in the calculation area of physical model [27, 28]. Considering the non-thermal equilibrium between gas and solid phases, and according to the mass conservation and energy in the micro-element body, the conservation law is used to establish the one-dimensional double temperature control equation for gas solid two phase.

The continuity equation is:

$$\frac{\partial(\varepsilon\rho_g)}{\partial t}+\frac{\partial(\varepsilon\rho_g)}{\partial x}=0 \tag{1}$$

The energy equation of mixed gases is:

$$\varepsilon\frac{\partial(C_{pg}\rho_g T_g)}{\partial t}+\varepsilon\frac{\partial(C_{pg}\rho_g uT)}{\partial x}=\varepsilon\frac{\partial}{\partial x}\left(\lambda_g\frac{\partial T_g}{\partial x}\right)+\varepsilon h_0 W-h_v(T_g-T_s) \tag{2}$$

The energy equation for porous medium is:

$$(1-\varepsilon)\frac{\partial(C_{ps}\rho_s T_s)}{\partial t}=\frac{\partial}{\partial x}\left(\lambda_s\frac{\partial T_s}{\partial x}\right)-\frac{\partial q_r}{\partial x}+h_v(T_g-T_s)-\xi(T_s-T_0) \tag{3}$$

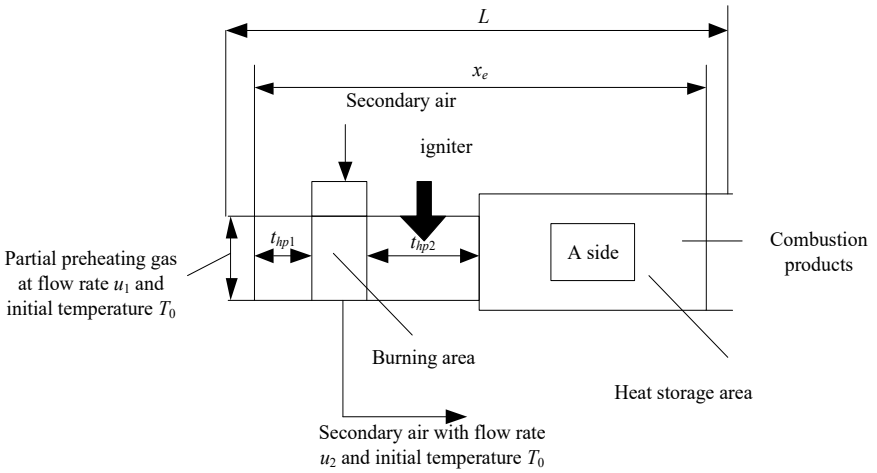

Figure 1. Physical model of reciprocating porous medium combustion system

The composition equation of the product is:

$$\frac{\partial(\rho_g Y)}{\partial t}+\frac{\partial(\rho_g u Y)}{\partial x}=\frac{\partial}{\partial x}\left(D\rho_g\frac{\partial Y}{\partial x}\right)+W \tag{4}$$

In the above equations, the porosity is ε; T is temperature; Y is product component; h_0 is low calorific value of fuel per unit mass; W is chemical reaction rate; λ_g is gas thermal conductivity; D is diffusion coefficient; C_{pg} is gas specific heat; C_{ps} is specific heat of porous medium; q_r is the radiation of porous medium; ξ is wall heat loss coefficient of combustion system; The subscripts is a porous medium, and the subscript g indicates gas.

λ_s is the thermal conductivity of solid, and it can be obtained by the following empirical equation.

$$\lambda_s=(1-\varepsilon)(0.561-0.855\log(T_s)) \tag{5}$$

h_v is the volumetric heat transfer coefficient, which is mainly obtained from the Nusselt number of dimensionless volume as following Equation (6):

$$Nu_{v,1}=\frac{h_v d_m^2}{\lambda_s} \tag{6}$$

The Nusselt number of dimensionless volume can be obtained by the following Equation (7):

$$Nu_{v,1}=\left(0.0426+\frac{1.236 d_m}{X_e}\right)/\mathrm{Re}_{dm} \tag{7}$$

The average pore size d_m and Reynolds number of aperture Re_{dm} is are obtained through the following Equation (8):

$$d_m=\sqrt{4\phi/\pi}\,/\,ppc;\mathrm{Re}_{dm}=\frac{u d_m^2}{\upsilon} \tag{8}$$

where ppc is the number of holes in porous medium in a centimeter unit length.

Similarly, the second half cycle is a heating process in which the secondary air flows backward from the downstream of the regenerator into the system. There is no combustion reaction, but a simple gas-solid two-phase heat transfer process [29]. Therefore, the model equation in the second half cycle can be further simplified as follows:

The continuity equation is:

$$\frac{\partial(\varepsilon\rho_g)}{\partial t}+\frac{\partial(\varepsilon\rho_g u_2)}{\partial x}=0 \tag{9}$$

The energy equation of mixed gases is:

$$\varepsilon\frac{\partial(C_{pg}\rho_g T_g)}{\partial t}+\varepsilon\frac{\partial(C_p\rho_g u_2 T_g)}{\partial x}=$$
$$\varepsilon\frac{\partial}{\partial x}\left(\lambda_g\frac{\partial T_g}{\partial x}\right)-h_v(T_g-T_s) \tag{10}$$

The energy equation for porous medium is:

$$(1-\varepsilon)\frac{\partial(C_{ps}\rho_s T_s)}{\partial t}=\frac{\partial}{\partial x}\left(\lambda_s\frac{\partial T_s}{\partial x}\right)-$$
$$\frac{\partial q_r}{\partial x}+h_v(T_g-T_s)-\xi(T_s-T_0) \tag{11}$$

2.2.2. Treatment of chemical reaction source term

The combustion reaction is a very rapid exothermic reaction. Natural gas is used as combustion gas, the main component is methane, the content of which is up to 90%. Because it combusts with a large amount of air to form a lean gas, the proportion of other components is smaller [30]. Therefore, the combustion of other components can be neglected and only the chemical reaction of methane combustion can be considered. The stoichiometric equation of chemical reaction can be expressed as follows:

$$CH_4+2\phi^{-1}(O_2+3.762N_2)\rightarrow$$
$$CO_2+2H_2O+2(\phi^{-1}-1)O_2+2\phi^{-1}3.76N_2 \tag{12}$$

The experimental analysis shows that the oxygen concentration in the gas is very high and the combustion efficiency is very high when combustion is carried out in a reciprocating porous medium burner, especially for lean gas fuel with low calorific value. Therefore, in the model calculation, the combustion reaction is considered to be complete [31, 32]. In addition, the purpose of chemical reaction item treatment is the main one. The effect of thermal effect caused by combustion reaction on temperature field is considered. According to Arrehnius law, the thermal effect caused by one-step reaction is the same as that caused by detailed reaction. Therefore, the overall one-step irreversible reaction can be used to simplify the combustion reaction. Since the combustion reaction is assumed to follow Arrehnius law, the chemical reaction rate equation is as follows:

$$W=A_f\rho_R(1-Y)\exp(-E/RT_R) \tag{13}$$

where, the chemical reaction frequency factor $A_f=2.6\times10^8 s^{-1}$, activation energy $E=130kJ/mol$.

Therefore, in combustion reaction, only the molar fraction of reactants and biomass components exists. Therefore, when the biomass component $Y<1$ or not equal to 1 in numerical simulation, it can be confirmed that combustion reaction can not proceed steadily.

2.2.3. Treatment of radiation source term

On the one hand, natural gas becomes a gas fuel with low calorific value after mixing with air, and the proportion of combustible gas component is relatively small [33]. Therefore, the proportion of triatomic radiative gases such as CO_2 and H_2O in the product is relatively small, and the radiation ability is greatly reduced. On the other hand, compared with the radiation effect of porous medium, the radiation effect of gas is much less than that of porous medium. The radiation effect of gas can be neglected. Only the radiation effect of solids is considered. At the same time, the radiation coefficient of foam ceramic medium and the phase function parameter fluctuate less with wavelength variation [34], so the wavelength effect can be considered as smaller, the wavelength is treated as gray body. For the micro-elements in the physical model area, the radiation energy transfer is established as follows:

$$\frac{\partial q_r(\tau)}{\partial x}=-2\pi k\Big[I_0E_2(\tau)+$$
$$I_e E_2(\tau_e-\tau)-2I_b(\tau)+\int_0^{\tau_e}I_b(\tau')E(|\tau-\tau'|)d\tau'\Big] \tag{14}$$

where, $I_b(\tau)$ and $E_n(\tau)$ respectively denote black body radiation intensity and n-order exponential integral function, as shown in Equation (15):

$$I_b(\tau)=\frac{\sigma T^4}{\pi};E_n(\tau)=\int_0^1\xi^{n-2}\exp(-\tau/\zeta)d\zeta \tag{15}$$

Porous ceramic foam is composed of a network framework with twelve sides interpenetrating. It has high randomness, uncertainty and complex structure. It can be treated as a continuous medium, and the combustion of porous medium makes the temperature distribution in the combustion chamber more uniform. The gap is much smaller, so that radiation mainly comes from the adjacent point, and the radiation energy far away has been greatly attenuated before reaching the micro-element [35]. Therefore, the radiation energy can be treated by the diffusion approximation method based on the optical thickness assumption, and the Rosseland diffusion equation can be obtained as follows:

$$q_r(x) = -\frac{16}{3}\frac{\sigma T^3}{k}\frac{dT}{dx} \tag{16}$$

The Stephen-Boltzmann constant $\sigma = 5.67\times10^{-8} W/m^2\cdot K$ and k is the radiation attenuation coefficient.

By incorporating the above equations into the energy equation of porous medium and combining them, the expression (17) of energy diffusion equation of porous medium can be obtained:

$$(1-\varepsilon)\frac{\partial(C_{ps}\rho_s T_s)}{\partial t} = \frac{\partial}{\partial x}(\lambda_{ss})\frac{\partial T_s}{\partial x} + h_v(T_g - T_s) \tag{17}$$

where

$$\lambda_{ss} = \lambda_s + \frac{16}{3}\frac{\sigma T_s^3}{k} \tag{18}$$

where, λ_{ss} is the effective conversion coefficient of heat conduction.

2.2.4. Establishment of ignition model

The reciprocating porous medium burner is ignited by an igniter. The ignition process is regarded as a uniform exothermic process with constant flow [36]. The uniform heat release rate is limited to the combustion area of porous medium, and the heat source range is 1/50 of the whole porous medium area. The corresponding model equation is simplified as the relative heat transfer between gas and solid with constant internal heat source [37]. The temperature at which the ignition is stabilized is the initial value of the ignition combustion as the mixed gas.

2.2.5. Initial boundary condition

1. Initial condition

When $t = 0, -0.05x_e < x \le L$, then:

$$T_g = T_s = T_{i0}; Y = 0; u = u_1 + u_2 \tag{19}$$

2. Boundary condition

The first half cycle $0 \le t \le t_{hp}, u > 0$, when $x = -0.05x_e$, then:

$$T_g = (1-\alpha)T_0 + \alpha T_{g2}; Y_{in} = 0; u = u_1 + u_2 \tag{20}$$

If $X = L$, there is:

$$\frac{\partial T_g}{\partial x} = \frac{\partial Y}{\partial x} = 0; u = u_1 + u_2 \tag{21}$$

If $x = 0$ and $x = 0$, there is:

$$(1-\varepsilon)\lambda_s\frac{\partial T_s}{\partial x} = -\alpha_s(T_g - T_s)\big|_{x=0} \tag{22}$$

α_s is the convection heat transfer coefficient, $\alpha_s = h_v / 169.4\,ppc$, and ppc is the number of hole per cm unit length.

The second half cycle $t_{tp} \le t \le 2t_{hp}, u < 0$, if $x = L$:

$$T_g = T_0; Y_{in} = 0; u = u_2 \tag{23}$$

If $x = -0.05x_e$, there is:

$$\frac{\partial T_g}{\partial x} = 0; u = u_2 \tag{24}$$

At $x = 0$ and $x = x_e$, there is:

$$(1-\varepsilon)\lambda_s\frac{\partial T_s}{\partial x} = -\alpha_s(T_g - T_s)\big|_{x=x_e} \tag{25}$$

3. Solid wall boundary

In order to prevent backfire, a cooling aluminium ring with a length of 40 mm is installed at the inlet of the premixed gas upstream of the burner. The heat loss coefficient ξ_1 is treated according to the unit length uniform heat sink, and 1 200 is selected through the comparison of the test results. Other avoiding areas adopt better thermal insulation measures in the test process, with less heat loss, according to adiabatic heat treatment.

2.2.6. Solution of mathematical model

Aiming at the established mathematical model equation, variable of that dimension is 1 and parameter of that dimension is 1 are introduced. The model equation and boundary conditions are transformed into two dimension 1 forms. The finite volume method is used to discretize the model equation, boundary condition and calculation area. The model equation is solved by Gauss-Seidel iteration method, and the combustion efficiency is obtained. The calculation results of the rate can effectively analyze the relationship between flow characteristics and efficiency of the reciprocating porous medium burner.

Firstly, ignition simulation is carried out. Given constant heat source h_0, the gas-solid two-phase energy equation of constant internal heat source is solved. The obtained temperature distribution field is taken as the initial ignition temperature, and then the numerical simulation of system combustion is carried out. Secondly, the position of the flame is not predetermined, but by the energy balance of the system itself.

$$\begin{aligned}
&X = x/x_e, \theta = T/T_0, \beta = ut/x_0, \tau_e = kx,\\
&\beta_{hp} = ut_{hp}/x_e, M_2 = x_e^{2\xi}/\lambda_g, \mathrm{Re} = ux_e v, \gamma_e = \lambda_s/\lambda_g\\
&\mathrm{Pr} = \rho_g v c_p/\lambda_g, Le = \rho_g c_p D/\lambda_g, hr = \rho_s C_s/\rho_g C_s,\\
&E_a = E/RT_0, R_s = A_f x_e/v, M = x_e^2 h_v\lambda_g, H_0 = h_0/c_p T_0,\\
&Nr = k\lambda_g/4\sigma T_0^3, Nu = \alpha_s x_e/(\lambda_s + 16\sigma T_s^3/3k)
\end{aligned} \tag{26}$$

In the above equation, X is the coordinate of that dimension is 1; E_a is the activation energy; θ is the temperature; Le is Levis number; D is diffusion coefficient; M is the convective heat transfer coefficient; v is motion viscosity.

3. Results

In order to verify the validity of the model of the relationship between flow characteristics and efficiency of reciprocating porous medium burner constructed in this paper, the application effect of the model is empirically

analyzed. The main characteristic of porous medium combustion is "superenthalpy combustion". The reciprocating thermal cycle porous medium combustion system is also based on porous medium combustion. Periodic reversing combustion achieves normal and stable operation. Therefore, in the steady combustion process of reciprocating porous medium burner system, there is also the phenomenon of "superenthalpy combustion". Superenthalpy combustion has the characteristics of high thermal efficiency and high combustion rate. The experiment will start from the flow characteristics of the burner, such as reversal half cycle, gas calorific value, secondary air ratio and so on to analyze the validity of the model.

The following characteristics are explained below. Relative to superenthalpy θ_r, a characteristic quantity used to represent the "superenthalpy" combustion program of a combustion system is defined by Hanamura, as shown in Equation (27):

$$\theta_r = \frac{\theta_{\max} - 1}{\theta_{th} - 1} \tag{27}$$

where, $\theta_{\max}$ represents the maximum temperature of reciprocating porous medium burner and θ_{th} represents the theoretical adiabatic temperature of gas. In the reaction model, only the products and reactants can be distinguished. Therefore, combustion efficiency η is directly represented by the biomass components calculated in the model. It should be pointed out that the model in this paper uses an irreversible reaction to approximate the combustion reaction effect of the system. The reaction model is relatively simple, only a simple qualitative analysis.

3.1. Impact analysis of commutation half cycle

In Figure 2, Reynolds number $\mathrm{Re} = 10321$, gas calorific value $H_0 = 3.48$, secondary air ratio $a = 0.2$, porosity in the left end burner is ε_1, and porosity in the right end burneris $\varepsilon_2 = 0.51$. When the heat loss coefficient in left end is 1200, the influence of commutation half cycle on relative enthalpy and combustion efficiency is analyzed by the proposed model. As shown in the figure, for the relative superenthalpy, the relative superenthalpy increases and the combustion efficiency increases with the increase of the commutation half cycle. It increases to the maximum at half cycle $\beta_{hp} = 40$ and then decreases gradually. This is because when the calorific value of the gas is the same, the maximum adiabatic theoretical combustion temperature remains unchanged. From the analysis of Figure 2, it can be seen that with the increase of half cycle, the maximum peak combustion temperature is relatively small at the beginning, relatively high at half cycle $\beta_{hp} = 40$, and then gradually decreases.

Generally speaking, the effect of commutation half cycle on relative superenthalpy is relatively small, it is equivalent to that of commutation half cycle on combustion efficiency of reciprocating porous medium burner, which is between 1.0 and 1.06. This is because when the calorific value of premixed gas is fixed, the heat released from combustion is fixed. Under normal combustion conditions, the change of commutation half cycle is only an external factor to change the maximum temperature of premixed gas combustion, not an internal factor, so the influence is relatively small.

For combustion efficiency, at half cycle $\beta_{hp} = 5$, it is relatively small, less than 0.9, and then increases rapidly, reaching a higher level after $\beta_{hp} = 40$, then decreases slightly, but the decrease is very small. Overall, except for the small commutation half cycle, the combustion efficiency is relatively low, and the overall combustion efficiency remains at a higher level. Therefore, the model can effectively analyze the relationship between commutation half cycle and combustion efficiency.

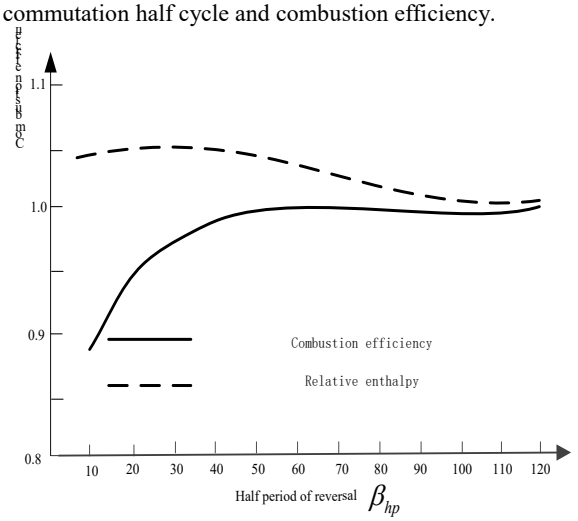

Figure 2. Effect of half-period of commutation on the combustion characteristics and efficiency of superenthalpy

3.2. Impact analysis of gas calorific value

Figure 3 shows the effect of gas calorific value on relative superenthalpy and combustion efficiency when Reynolds number $\mathrm{Re} = 10321$, half cycle $\beta_{hp} = 40$, secondary air ratio $a = 0.2$, porosity in the left end burner is $\varepsilon_1 = 0.85$, porosity in the right end burner is $\varepsilon_2 = 0.51$ in and heat loss coefficient in left end is 1200, the influence of gas calorific value on the relative super-energy and combustion efficiency is obtained from the model analysis in this paper. As shown in the figure, for the relative superenthalpy, the relative superenthalpy decreases rapidly with the increase of the calorific value of the gas. When the calorific value of the gas is $H_0 = 3.48$, the relative superenthalpy basically approaches 1, and the hyperbolic trend is obvious. The results show that with the increase of calorific value of gas, the characteristic of "superenthalpy combustion" decreases gradually, and the lower the calorific value of gas is, the more obvious the phenomenon of "superenthalpy combustion" is.

For combustion efficiency, with the increase of calorific value of gas, combustion efficiency gradually increases, and overall, combustion efficiency remains at a high level. This is because when the calorific value of the gas $H_0 = 0.8$, the peak value of the maximum combustion temperature is smaller, the temperature distribution presents an inverted "V" distribution, the burner has been in the extreme lean combustion state, and the combustion efficiency is relatively low; With the increase of the calorific value, the overall temperature level in the system increases, the peak temperature gradually increases, and the combustion efficiency gradually increases. Therefore, this model can

effectively analyze the relationship between gas calorific value and combustion efficiency.

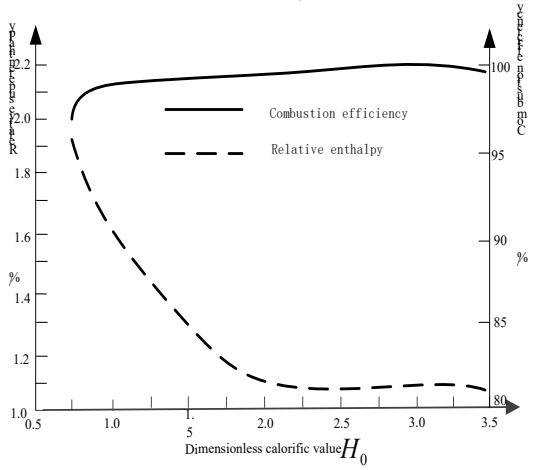

Figure 3. Influence of gas calorific value on superenthalpy combustion characteristics and combustion efficiency

3.3. Impact analysis of the secondary air ratio

Figure 4 shows the effect of secondary air ratio on relative superenthalpy and combustion efficiency when Reynolds number is $\mathrm{Re} = 10321$, gas calorific value is $H_0 = 2.27$, half cycle is $\beta_{hp} = 40$, porosity in the left end burner is $\varepsilon_1 = 0.85$, porosity in the right end burner is $\varepsilon_2 = 0.51$ and heat loss coefficient in left burner is 1200. As shown in the figure, for the relative superenthalpy, the relative superenthalpy is lower when the secondary air ratio is $a = 0.1$. When $a = 0.2$, the relative superenthalpy is higher, then decreases gradually. With the increase of the secondary air ratio, the maximum combustion peak temperature is higher when the secondary air ratio is $a = 0.2$, then decreases gradually, while the adiabatic theoretical combustion temperature of gas combustion is fixed. Therefore, the variation of relative superenthalpy is similar to that of maximum combustion peak temperature. At the beginning, the secondary air ratio is relatively high when $a = 0.2$, and then decreases gradually.

For combustion efficiency, similar to the relative enthalpy, it is relatively small when the secondary air ratio is a = 3 and relatively high when the secondary air ratio is a = 1, and then gradually decreases. The main reason is the analysis of the influence of the two wind ratio on the combustion temperature distribution. Therefore, this model can effectively analyze the relationship between the two air ratio and combustion efficiency.

For combustion efficiency, similar to the relative superenthalpy, it is relatively small when the secondary air ratio is $a = 0.1$ and relatively high when the secondary air ratio is $a = 0.2$, and then gradually decreases. The main reason is the analysis of the influence of the secondary air ratio on the combustion temperature distribution. Therefore, this model can effectively analyze the relationship between the secondary air ratio and combustion efficiency.

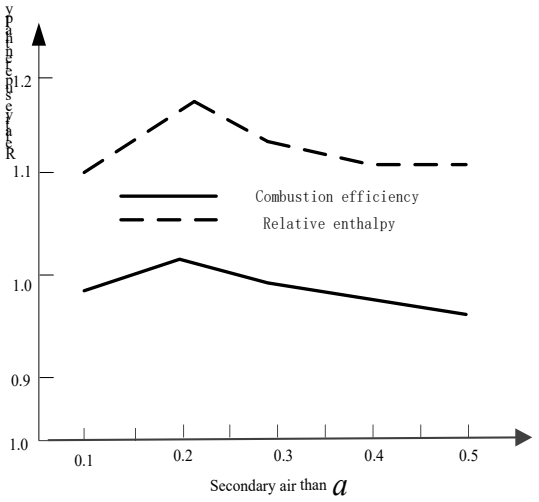

Figure 4. Influence of secondary air ratio on combustion characteristics and combustion efficiency

3.4. Influence analysis of reynolds number

Figure 5 shows the effect of Reynolds number on relative superenthalpy and combustion efficiency of the burner system when the calorific value of gas is $H_0 = 13.4$, half cycle is $\beta_{hp} = 40$, secondary air ratio is $a = 0.2$, porosity in the left burner is $\varepsilon_1 = 0.85$, porosity in the right burner is $\varepsilon_2 = 0.51$ and heat loss coefficient is 1200 in the left. As shown in the figure, with the increase of Reynolds number, the relative superenthalpy increases obviously and shows a linear distribution relationship. The main reason is that when the calorific value of the gas is constant, the adiabatic theoretical combustion temperature of the gas remains unchanged. With the increase of Reynolds number, the combustion load of the system increases correspondingly, the maximum peak temperature increases gradually, and the relative enthalpy increases gradually, showing an approximate linear relationship.

For the combustion efficiency, similar to the relative superenthalpy, the combustion efficiency increases slightly with the increase of Reynolds number, and overall, the change is relatively small. With the increase of Reynolds number, the maximum combustion temperature and preheating zone temperature gradually increase, the preheating effect of fresh gas gradually increases, the combustion effect in high temperature zone increases, and the combustion efficiency gradually increases. Overall, the combustor combustion efficiency is very high, basically maintained at more than 98%.

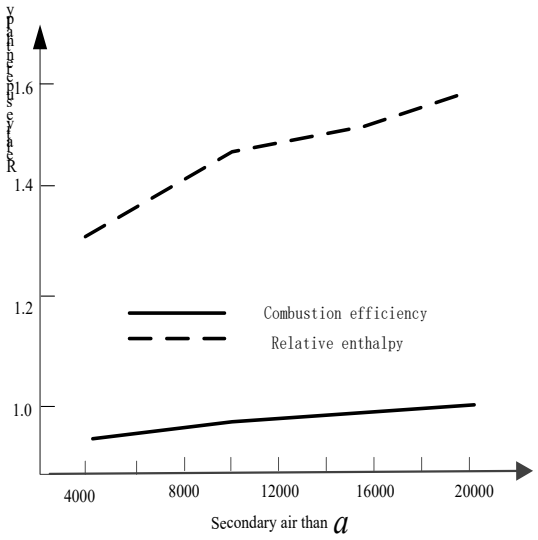

Figure 5. Effects of reynolds number on combustion characteristics and efficiency of superenthalpy

3.5. Comparison analysis of time-consuming

In order to verify the efficiency and stability of the model, the results of the flow characteristics and efficiency relationship model of reciprocating porous medium burner based on energy spectrum analysis are compared. The time-consuming results of analyzing the relationship between reversal half-cycle, gas calorific value, secondary air ratio and Reynolds number and combustion efficiency by the two models are compared. The time-consuming results of analyzing the relationship between flow characteristics and combustion efficiency of reciprocating porous medium burner by using the present model and the model based on energy spectrum analysis are shown in Tables 1 and 2, respectively.

Table 1. Results for the model in this article (s)

	Half period of reversal	Gas calorific value effect	Secondary air than	Reynolds number
1	0.36	0.42	0.41	0.42
2	0.42	0.35	0.47	0.5
3	0.35	0.36	0.4	0.39
4	0.47	0.42	0.42	0.39
5	0.52	0.36	0.43	0.42
6	0.32	0.33	0.44	0.45
7	0.25	0.36	0.45	0.44
8	0.36	0.36	0.48	0.35
9	0.35	0.38	0.26	0.32
10	0.41	0.35	0.41	0.31
11	0.47	0.41	0.35	0.36
12	0.45	0.4	0.38	0.28
13	0.43	0.37	0.36	0.35
14	0.42	0.38	0.24	0.41
15	0.41	0.38	0.35	0.26

The results of Table 1 show that the overall analysis of the relationship between flow characteristics and efficiency of reciprocating porous medium burner in the proposed model takes less time than 0.5 s, the stability of this model is strong according to the results of many measurements, and the difference between the measurements is small.

Table 2. Time-use results of flow characteristic and efficiency model of reciprocating porous medium burner based on energy spectrum analysis (s)

	Half period of reversal	Gas calorific value effect	Secondary air than	Reynolds number
1	3.25	3.26	3.46	2.25
2	3.24	3.26	4.25	2.54
3	5.24	2.35	4.25	2.45
4	2.31	2.36	4.36	2.65
5	1.35	2.47	4.36	2.15
6	2.56	2.58	4.28	2.35
7	1.24	2.65	2.57	2.65
8	1.35	2.64	2.56	2.58
9	2.55	2.35	2.68	2.57
10	2.65	3.16	2.69	2.65
11	2.24	3.25	2.34	2.45
12	2.73	3.16	2.65	2.35
13	2.71	3.25	2.58	2.35
14	2.67	3.28	2.26	2.45
15	3.26	3.26	2.34	2.65

From the data in Table 2, it can be seen that the relationship between flow characteristics and efficiency of reciprocating porous medium burner based on energy spectrum analysis takes longer time to analyze the relationship between flow characteristics and efficiency of reciprocating porous medium burner than that of the model in this paper. The stability of the model can be seen from many measurements. The difference between two adjacent analyses is relatively high. Therefore, the results of Tables 1 and 2 show that the model presented in this paper has strong stability and high efficiency in analyzing the relationship between flow characteristics and efficiency of reciprocating porous medium.

Comprehensive analysis of experimental results shows that the model can effectively analyze the relationship between flow characteristics and efficiency of reciprocating porous medium burner, and the stability and efficiency of the model is high, which has strong practicability.

4. Discussion

For the application of new combustion technology, a large number of experimental studies are needed, and the combustion mechanism and flow characteristics should be analyzed so that it can be applied to industry. The premixed combustion of porous medium gas should be further studied in the following aspects.

1. Gas adaptability: It is not difficult to find that the existing research results are mainly focused on the numerical simulation and experiment of a single gas source. Most of them are natural gas, a small part is liquefied petroleum gas, and the combustion stability of artificial gas with high tempering tendency in porous medium. Qualitative research on combustion

characteristics has not been reported. Only the numerical simulation of the effect of hydrogen addition on Methane combustion in porous medium has been made. The results show that the lean combustion limit is enlarged and the combustion speed is doubled after hydrogenation, but the results are not validated by experiments.

2. Theoretical study of porous medium gas combustion-heat transfer combined device with built-in cold source: When heat exchanger is installed in the combustor, the combustion stability of the high combination device is new and different from that of the combustor only, and the research results of foreign scholars are quite inconsistent. Scholars in China have not done any detailed research in this respect. Therefore, it is necessary for us to study the feasibility and reliable common stable working range of using multiple gas sources according to the characteristics of gas supply in China.

Academically, through research, we can deepen our understanding of the complex physical and chemical phenomena of porous medium combustion after the built-in cold source, and clarify the combustion characteristics of porous medium, including flame stability. The influence of pollutant emission promotes the interdisciplinary integration of porous medium combustion, radiation heat transfer, chemical reaction dynamics and other disciplines, and innovates while tracking the international academic frontiers.

3. Equipment development: Taking porous medium combustion device without or without built-in cold source as object, a lot of research has been carried out from theory to experiment, such as the mechanism and characteristics of heat transfer enhancement, combustion stability, pollutant emission, etc., so as to develop ultra-miniaturized gas combustion equipment or combustion heat transfer combination device.

5. Conclusions

In this paper, a new model to study the relationship between flow characteristics and efficiency of reciprocating porous medium burner is presented. Based on the structural symmetry of reciprocating porous medium burning system and the periodic exchange of internal gas flow, the physical model of reciprocating thermal cycle porous medium burning system is determined. On this basis, the reciprocating porous medium burning system is constructed. The mathematical model of flow characteristics and efficiency of medium burner is established, and the normalization and solution of the model are designed. The relationship between flow characteristics and efficiency of reciprocating porous medium burner is analyzed effectively. From the experimental results, it can be concluded that the model can better analyze the relationship between the communication half cycle, gas calorific value, secondary air ratio and Reynolds number and combustion efficiency and combustion rate in reciprocating porous medium burner. The model also changes below 0.5 s when used. The reciprocating porous medium burner flow based on energy spectrum analysis is adopted. The relationship model between dynamic characteristics and efficiency is used to analyze the relationship between flow characteristics and efficiency of reciprocating porous medium burner. The time consumed in this model is more than 2 seconds longer than that in the proposed model. It shows that the proposed model has high analysis efficiency and practicability.

References

[1] Losi, G.; Arnone, D.; Correra, S. Modelling and statistical analysis of high viscosity oil/air slug flow characteristics in a small diameter horizontal pipe. Chemical Engineering Science, 2016, 148: 190-202.

[2] Hunt, J.E.A.; Stodart, C.; Ferguson, R.A. The influence of participant characteristics on the relationship between cuff pressure and level of blood flow restriction. European Journal of Applied Physiology, 2016, 116: 1421-1432.

[3] Liu, Y.; Mutailipu, M.; Jiang, L. Interfacial tension and contact angle measurements for the evaluation of CO2-brine two-phase flow characteristics in porous media. Environmental Progress & Sustainable Energy, 2016, 34: 1756-1762.

[4] Akselsen, A.H. Characteristic methods and Roe's method for the incompressible two-fluid model for stratified pipe flow. International Journal of Multiphase Flow, 2017, 89: 81-91

[5] Xie, P.; Lu, X.; Yang, X. Characteristics of liquid flow in a rotating packed bed for CO_2, capture: A CFD analysis. Chemical Engineering Science, 2017, 172: 216-229.

[6] Nam, J.S.; Lee, M.Y.; Seo, J.H. Numerical analysis on the electrical and thermal flow characteristics of Ar-N 2. Inductively Coupled Plasma Torch System. Journal of the Korean Physical Society, 2018, 72: 755-764.

[7] Wang, Y.; Cao, L.; Hu, P.; Li, B.; Li, Y. Model establishment and performance evaluation of a modified regenerative system for a 660 MW supercritical unit running at the IPT-setting mode. Energy, 2019, 179: 890-915.

[8] Wen, B.Z.; Yong, Y.; Yong, R.Y. Measurement of flow characteristics in a bubbling fluidized bed using electrostatic sensor arrays. IEEE Transactions on Instrumentation and Measurement, 2016, 65: 703-712.

[9] Wang, C.; Zheng, D.; Zhang, Y. Relationship between lightning activity and vertical airflow characteristics in thunderstorms. Atmospheric Research, 2017, 191: 12-19.

[10] Łukasz, A. Influence of geometrical parameters on the flow characteristics of multi-pipe earth-to-air heat exchangers-experimental and CFD investigations. Applied Energy, 2018, 226: 849-861.

[11] Yu, S.; Wang, J.; Yan, M. Experimental and numerical study on single-phase flow characteristics of natural circulation system with heated narrow rectangular channel under rolling motion condition. Annals of Nuclear Energy, 2017, 103: 97-113.

[12] Wang, G.; Wang, F.; Shen, F.; Jiang, T.; Chen, Z.; Hu, P. Experimental and optical performances of a solar CPV device using a linear Fresnel reflector concentrator. Renewable Energy, 2020, 146: 2351-2361.

[13] Sun, F.; Yao, Y.; Li, X. The flow and heat transfer characteristics of superheated steam in offshore wells and analysis of superheated steam performance. Computers & Chemical Engineering, 2017, 100: 80-93.

[14] Zoca, S.M.; Shafii, B.; Price, W.J. Use of principal component analysis to evaluate variability in CASA and flow cytometer sperm characteristics. Animal Reproduction Science, 2018, 194: e20-e21.

[15] Wang, Y.; Shukla, A.; Liu, S. A state of art review on methodologies for heat transfer and energy flow characteristics of the active building envelopes. Renewable & Sustainable Energy Reviews, 2017, 78: 1102-1116.

[16] Wan Mahari, W.A.; Chong, C.T.; Cheng, C.K.; Lee, C.L.; Hendrata, K.; Yek, P.N.Y.; Ma, N.L.; Lam, S.S. Production of

value-added liquid fuel via microwave co-pyrolysis of used frying oil and plastic waste. Energy, 2018, 162: 309-317.

[17] Zalucky, J.; Claußnitzer, T.; Schubert, M. Pulse flow in solid foam packed reactors: Analysis of morphology and key characteristics. Chemical Engineering Journal, 2017, 307: 339-352.

[18] Romero, G.; Panzalis, R.; Ruegg, P. Relationship of goat milk flow emission variables with milking routine, milking parameters, milking machine characteristics and goat physiology. Animal, 2017, 11: 1-6.

[19] Jin, Z.J.; Chen, F.Q.; Qian, J.Y. Numerical analysis of flow and temperature characteristics in a high multi-stage pressur14e reducing valve for hydrogen refueling station. International Journal of Hydrogen Energy, 2016, 41: 5559-5570.

[20] Parziale, N.; Adhikari, R. Model and sensitivity analysis of the reciprocating biomass conversion reactor (RBCR). International Journal of Heat and Mass Transfer, 2020, 147: 118988.

[21] Batista, M.R.; Mota, J. Monotone iterative method of upper and lower solutions applied to a multilayer combustion model in porous media. Nonlinear Analysis Real World Applications, 2021, 58(3): 103223.

[22] Quaye, E.K.; Pan, J.; Zhang, Y.; Lu, Q.; Alubokin, A.A. Effects of influencing factors on premixed CH4-O2 combustion in a cylindrical porous media combustor. Chemical Engineering and Processing, 2021, 161(5-6): 108320.

[23] Devi, S.; Sahoo, N.; Muthukumar, P. Effect of combustion zone material on the thermal performance of a biogas-fuelled porous media burner: Experimental studies. Biomass Conversion and Biorefinery, 2020, 175: 1-9.

[24] Dowd, C.S.; Meadows, J.W. Thermoacoustic instability model with porous media: linear stability analysis and the impact of porous media. Journal of Engineering for Gas Turbines and Power, 2019, 141(4): 041017.

[25] Bai, X. Eight energy and material flow characteristics of urban ecosystems. Ambio, 2016, 45: 819-830.

[26] Cebral, J.R.; Duan, X.; Gade, P.S. Regional mapping of flow and wall characteristics of intracranial aneurysms. Annals of Biomedical Engineering, 2016, 44: 1-15.

[27] Alzoubi, K. Parametric study for a reciprocating screw blow injection molding process using design of experiments tools. Jordan Journal of Mechanical and Industrial Engineering, 2016, 10(4): 279-284.

[28] Yang, S.; Cahyadi, A.; Wang, J. DEM study of granular flow characteristics in the active and passive regions of a three-dimensional rotating drum. Aiche Journal, 2016, 62: 3874-3888.

[29] Zhang, B.; Ren, Z.; Shi, S. Numerical analysis of gasification and emission characteristics of a two-stage entrained flow gasifier. Chemical Engineering Science, 2016, 152: 227-238.

[30] Jiang, Y.; He, M.H.; Yu, C.L. Modeling and analysis of deceptive jamming signal based on phase quantization DRFM. Journal of China Academy of Electronics and Information Technology, 2015, 10: 361-366.

[31] Xu, J.Z.; Zhao, C.Y.; Ji, Y.K. Research on modelling and fast simulation of cascaded two-level converter. Journal of Power Supply, 2015, 13: 101-109.

[32] Ravi Kumar, S. The effect of the couple stress fluid flow on MHD peristaltic motion with uniform porous medium in the presence of slip effect. Jordan Journal of Mechanical and Industrial Engineering, 2015, 9(4): 269-278.

[33] Zhou, H.D.; Zhang, D.Z.; Gong, H. Analyzing and modeling for charging/discharging process of substation battery. Chinese Journal of Power Sources, 2015, 39: 536-538.

[34] Zhang, S.J. The Research on mathematical modeling education contest based on IT technology. Automation & Instrumentation, 2016, (4): 126-127.

[35] Peng, F.S. Basketball player overtraining modeling and simulation to elbow knee joint injury. Computer Simulation, 2015, 32: 382-385.

[36] Cheng, Y.W.; Ng, K.H.; Lam, S.S.; Lim, J.W.; Wongsakulphasatch, S.; Witoon, T.; Cheng, C.K. Syngas from catalytic steam reforming of palm oil mill effluent: An optimization study. International Journal of Hydrogen Energy, 2019, 44: 9220-9236.

[37] Shahirah, M.N.N.; Gimbun, J.; Lam, S.S.; Ng, Y.H.; Cheng, C.K. Synthesis and characterization of a La-Ni/alpha-Al2O3 catalyst and its use in pyrolysis of glycerol to syngas. Renewable Energy, 2019, 132: 1389-1401.